Available online at www.sciencedirect.com
SCIENCE DIRECT®
Chemical Physics Letters 386 (2004) 233–238
CHEMICAL PHYSICS LETTERS
www.elsevier.com/locate/cplett

Permeation dynamics of chloride ions in the ClC-0 and ClC-1 channels

Ben Corry *,[1], Megan O'Mara, Shin-Ho Chung *

Department of Theoretical Physics, Research School of Physical Sciences and Engineering, Australian National University, Canberra, ACT 0200, Australia

Received 16 December 2003; in final form 19 January 2004
Published online: 11 February 2004

Abstract

We examine the mechanisms underlying the transport of ions across ClC-0 and ClC-1, the two best characterized members of the ubiquitous ClC chloride channel family. Using molecular and Brownian dynamics techniques we create an open channel structure, deduce the permeation characteristics, and highlight the amino acid residues responsible for the different conductance properties of these channels.

The ClC family of chloride channels is widely distributed in the membranes of prokaryotic and eukaryotic cells and performs diverse physiological roles, from the control of cellular excitability, acidification of intracellular vesicles, to the regulation of cell volume [1–3]. However, the dynamics of Cl^- permeation through these channels are not fully understood. We examine the mechanisms underlying the transport of ions across ClC-0, found in the electric organ of *Torpedo* [4], and ClC-1, the muscle chloride channel, mutations of which cause myotonia in mice [5] and humans [6]. Biophysical studies reveal that these channels undergo voltage-dependent transitions between open and closed states [7–9], gating being strongly facilitated by Cl^- ions in the extracellular solution. It is believed that an extracellular Cl^- ion entering the pore displaces the side-chain of a glutamate residue (Glu 148) that is blocking the ion pathway, creating an open state and thus enabling conduction to occur [10,11]. Analysis of the conduction processes in ClC-0 in a mixture of Cl^-/NO_3^- indicates that the permeation of ions takes place in a pore that is normally occupied by two or more ions [8]. Also, the conduction properties differ among the isoforms. For example, the current-voltage relationship measured from ClC-0 is linear [4], whereas it is inwardly rectifying in ClC-1 [9,12]. To understand these properties, we create open state structures of ClC-0 and ClC-1 using the crystal structure of the prokaryotic EcClC Cl^- channel as a basis. We then investigate the steps involved in ion permeation and the characteristics of the current–voltage curves using electrostatic calculations and three-dimensional Brownian dynamics simulations. Our results highlight the amino acid residues responsible for the different conductance properties of ClC-0 and ClC-1 and explain many experimental observations.

The crystal structures of the *Escherichia coli* ClC channel reported by Dutzler et al. [10,11] represent the wild-type channel in a closed state and the E148A mutant channel in a postulated open state. The ClC protein is a dimer, forming two identical pores, but we deal with only one of these throughout this study. A crosssection of this channel, with the front half of the protein removed, is shown in Fig. 1a. The protein has no continuous conduit from one side of the membrane to the other that is wide enough to accommodate ions. However a clear depression is apparent on each side of the protein, indicating the likely entrances to the pore. In the E148A mutant channel these two entrances are

* Corresponding authors. Fax: +61-893-801-005. (B. Corry).
E-mail addresses: ben@theochem.uwa.edu.au (B. Corry), shin-ho.chung@anu.edu.au (S.-H. Chung).
[1] Department of Chemistry, University of Western Australia, Crawley, WA, Perth 6009, Australia.

0009-2614/$ - see front matter © 2003 Elsevier B.V. All rights reserved.
doi:10.1016/j.cplett.2004.01.072

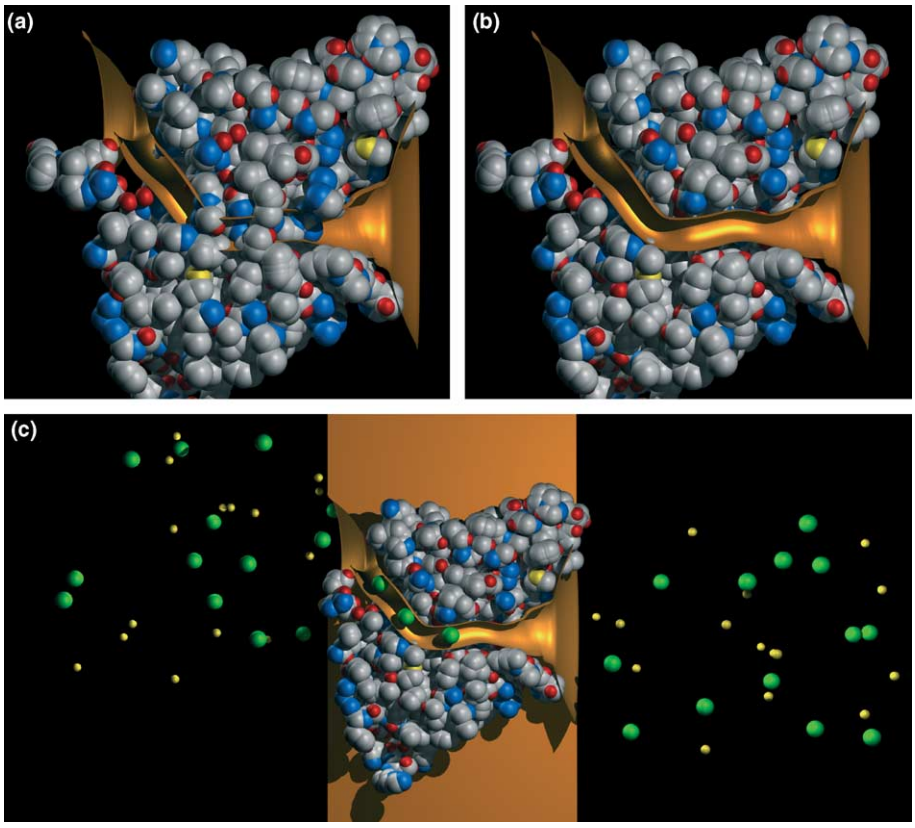

Fig. 1. The shape of the model channel and Brownian dynamics simulation system. The atomic detail of the crystal structure of *E. coli* ClC channel [10,11] (a) and the open state model of the channel (b) are shown with the front half of the atoms removed to illustrate the pore. The surface of our open pore (gold) is superimposed on each diagram. For the system used for Brownian dynamics simulations (c), the protein is incorporated in a low dielectric region representing the membrane (gold), and Cl^- (green) and Na^+ (yellow) ions are added to reservoirs on each end.

joined by a continuous pathway although it is still not quite wide enough to allow ions to pass through. In this structure, the pore contains three Cl^- ions so that the likely path of chloride ions through the pore can easily be determined. In the native x-ray structure two residues (Ser 107 and Glu 148) appear to completely occlude the pore in the closed state, while they partially occlude the pore in the postulated open state of the E148A mutant. Thus, the simplest method of creating a pore wide enough to pass a chloride ion in either structure is to move these residues sideways, away from the location of a permeating ion. We transform the occluded pore of the bacterial ClC channel into an open structure by moving as few atoms as possible away from the central pore region. We then assume that this general structure is the same in ClC-0 and ClC-1 and simply replace the non-conserved residues on this template to create open structures of the different channel isoforms.

We create approximate open structures of the EcClC pore starting from both the native and E148A mutant structures. Although larger structural changes may occur, we here create an open channel by moving as few atoms as possible. We expand the EcClC conduction pathway (PDB identification numbers 1KPK and 1OTS) to an open state by moving the atoms blocking the pore sideways using molecular dynamics simulations carried out with CHARMM v28b1, utilizing version 19 extended-atom parameters for proteins. A set of cylinders of radius 5 Å were set at six points near the center line of the pore containing the blocking atoms. Atoms inside the cylinders were pushed outward with harmonic force of 85 kT/Å^2, while all other atoms were held near their initial positions using comparatively weak harmonic constraints of 1.6 kT/Å^2. This resulted in a channel with a minimum radius of ≈2.5 Å, which is the smallest radius that would allow permeation of both Cl^- and NO_3^- through the channel. The resulting open structure is shown in Fig. 1b. The wall of the open pore shape used throughout our simulations is indicated by the gold-colored surface superimposed on the atomic structures. The open structures obtained starting from the native and mutant channels are almost identical, with a root-mean-square difference in atomic positions between the two being only 1.0 Å. In all the studies reported here we use the open channel coordinates determined from the native x-ray structure, however, we find we can replicate all these within the uncertainty limits when using the open channel structure created from the mutant channel. The open channel depicted in Fig. 1b illustrates that the ClC pore is not axially

symmetric like the well known KcsA potassium channel, but meanders through the protein.

As there is virtually no physiological data available on the EcClC channel (most likely due to its very small conductance) we concentrate on ClC-0 and ClC-1, the most well characterised ClC isoforms. We make the assumption that the overall structure of these channels is the same as that of EcClC. This seems to be a plausible assumption and gains support from a recent study that examines the location of inhibitor binding sites to demonstrate a high degree of structural similarity between bacterial and mammalian ClC channels [13]. The

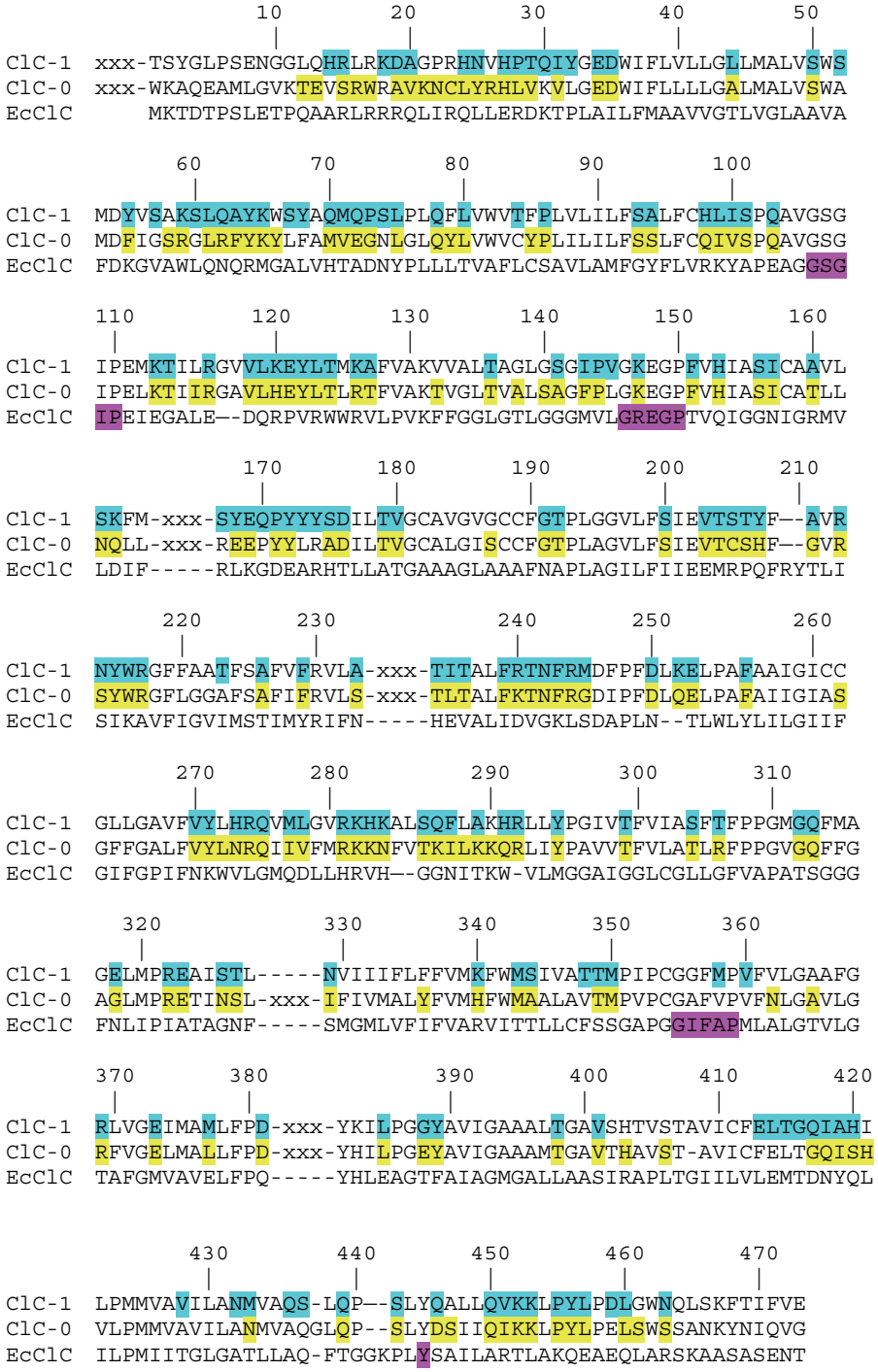

Fig. 2. The sequence alignment used for creating the ClC-0 and ClC-1 models. Residues altered to convert our EcCLC model to ClC-0 (i.e., only non conserved charged, dipolar and pore lining residues) are highlighted in yellow and those used to convert to ClC-1 in blue. For reference, the residues claimed by Dutzler et al. [10,11] to lie in the selectivity filter are highlighted in pink.

sequence alignments used to convert EcCLC to ClC-0 and ClC-1 are generated using the ClustalW web site [14] with a small amount of manual adjustment to gain the greatest alignment, and are shown in Fig. 2. Although ClC-0 shares only 24% sequence identity with EcCLC, and ClC-1 only 20%, if we consider residues of the same family rather than strict identity the homology rises to nearly 58% between the different isoforms. To convert EcClC to ClC-0 only non-conserved charged, dipole-containing and pore-lining amino acid residues are replaced. To do this we made 173 substitutions, three insertions and five deletions, and the residues involved are highlighted in Fig. 2. The corresponding numbers to mutate the prokaryotic ClC channel to ClC-1 are 179, 3 and 6, using the sequence alignment of Dutzler et al. [10]. To avoid confusion, we use the bacterial ClC numbering system throughout this paper for the aligned sequences. Notably, if we use the alignment directly from ClustalW (without manual adjustment) we find the channel barely conducts and that we cannot reproduce the experimental data.

To investigate the permeation process in ClC-0 and ClC-1, we solve Poisson's equation [15] to determine the energy required for ions to move through the channel. In the presence of a −80 mV applied potential, a Cl^- ion moving through the channel pore encounters a deep energy of approximately 47 kT in ClC-0 and 52 kT in ClC-1 ($1\ kT = 4.11 \times 10^{-21}$ J), created by the excess of positively charged residues lining the channel wall. In contrast, a Na^+ or K^+ ion entering the pore will face an energy barrier of approximately equal magnitude, effectively excluding it from the channel. The energy well seen by Cl^- is deep enough to accommodate two ions in a stable equilibrium, which is disrupted when a third ion enters the channel. With three ions in the channel, the depth of the energy well experienced by the outermost ion is reduced to about 11 kT. The ion can occasionally surmount this residual barrier through its random motions, aided by the Coulomb repulsion of the other ions, allowing it to move into the extracellular space. Thus, we deduce that the channels normally cradle two Cl^- ions and conduction takes place when a third ion enters the channel.

We determine the current–voltage curves by incorporating the atomic models into 3-dimensional Brownian dynamics simulations (see Fig. 1c), a technique that has been successfully used to describe ion permeation ion potassium [16], calcium [17] and other channels. In these we place 15 Cl^- ions and 15 Na^+ ions at a concentration of 150 mM in reservoirs at each end of the channel and simulate their motion due to the electric and random forces using the Langevin equation [18]. (The ionic diffusion constants are reduced from the bulk values by 50% in the pore, as determined with molecular dynamics studies by Allen et al. [19].) In Fig. 3, the current–voltage curves for ClC-0 (a) and ClC-1 (b) are illustrated. The ClC-0 curve (filled circles) is linear through the origin for applied potentials between −70 and +140 mV. Our simulated data shows excellent agreement with corresponding experimental measurements reported by Miller [4], which are superimposed (open circles). The core conductance is 11.3 ± 0.5 pS, compared to the experimental value of 9.4 ± 0.1 pS. In contrast, the inward and outward currents of ClC-1 are pronouncedly asymmetrical (Fig. 3b). The conductance at −100 mV is 1.0 pS, much smaller than in ClC-0. At positive voltages, the current across ClC-1 is less than 0.01 pA, until the driving force is increased to +160 mV. There are several whole-cell current measurements demonstrating that the ClC-1 channel is inwardly rectifying [9,12,20,21], as shown in the inset of Fig. 3b, but no single channel current–voltage curve for ClC-1 has

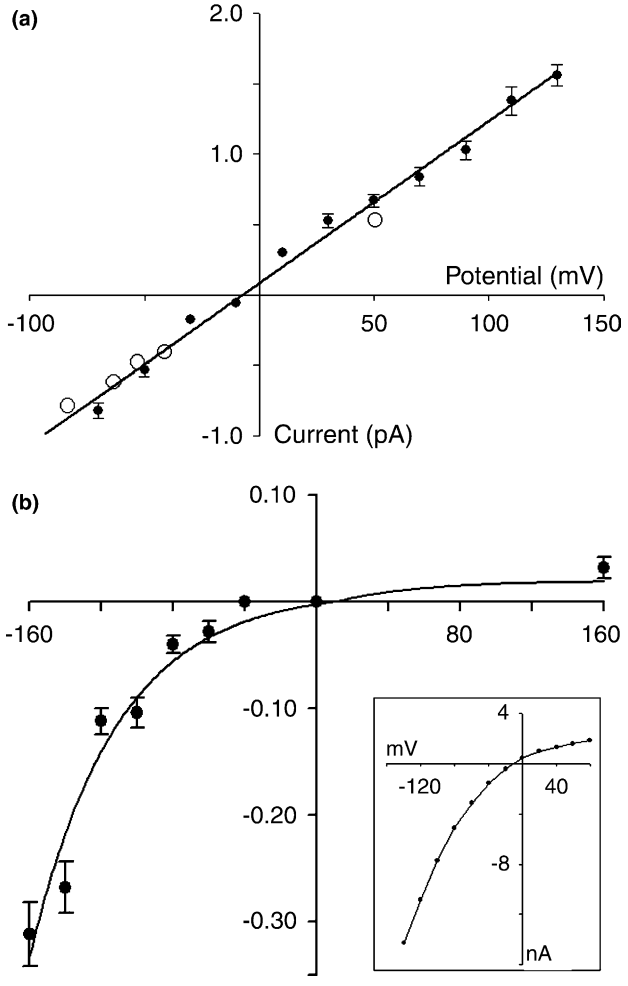

Fig. 3. Current–voltage curves for ClC-0 (a) and ClC-1 (b) determined from Brownian dynamics simulations. Simulations lasting between 8.4 and 22.4 μs, are performed with 150 mM symmetric ionic concentrations in the two reservoirs. Experimental results of Miller [4] for ClC-0 (open symbols) are superimposed on the simulated data (filled circles). The current–voltage curve obtained from whole-cell current [12] is reproduced in the inset of (b).

been published. Using low intracellular pH, which causes a slowing of gating kinetics, Saviane et al. [22] determined the channel conductance to be about 1.2 pS. This value is in close agreement with that determined by using concatemeric channels containing one subunit each of ClC-0 and ClC-1 [23]. Both the shape of the current–voltage relationship and the inward conductance determined from our simulation correspond with the experimental findings.

Brownian dynamics simulations also reveal the steps involved in ion permeation. In Figs. 4a and b we divide the channels into 100 layers and calculate the average number of ions in each during a simulation. In both cases, two ions dwell preferentially on the intracellular side of the channel. The equilibrium positions for ClC-0 are at $z = -11.0$ and -4.4 Å, near positively charged residues, Lys 452 and Lys 131, and those for ClC-1 are at $z = -7.7$ and 0 Å, near Lys 131 and Lys 147 (using the EcClC sequence numbering system). In the dwell histogram obtained from ClC-1, there is also a prominent peak at $z = -13.4$ Å, indicating that a third ion spends considerable time in the channel before a successful conduction event occurs. Notably, the location of the three peaks in ClC-1 correspond to the position of the three chloride ions in the crystal structure of the E148A channel [11]. In comparison, the position of the two peaks in ClC-0 are shifted slightly towards the intracellular side of the channel relative to the two innermost Cl^- ions in the E148A channel [11]. This shift reflects the presence of an additional negatively charged residue, Arg 62, lining the extracellular pore of ClC-0 and attracting Cl^- ions deeper into the channel.

With an applied potential of −80 mV, we find that there are almost 2.3 ions on average in the ClC-0 channel, demonstrating a third ion is needed for conduction and supporting the experimental evidence that the ClC-0 pore is occupied by at least two Cl^- ions [8]. In Fig. 4c we illustrate the steps involved in ion permeation through ClC-0. With two ions in the channel and a −80 mV potential, it takes around 125 ns before a third ion enters the channel. When three ions are in the narrow intracellular segment of the pore, the outermost Cl^- ion crosses the center of the channel, assisted by the Coulomb repulsive force. This step takes ~70 ns.

Similarly, the conduction process in ClC-1 also involves 3 ions, with the channel holding an average of 2.9 chloride ions. In ClC-1, ions have great difficulty in crossing the extracellular half of the channel, resulting in a low current. At −80 mV it takes about 1 μs for the outermost ion to climb this barrier. An examination of the amino acid sequence in ClC-0 and ClC-1 indicates that the differences observed are probably caused by an

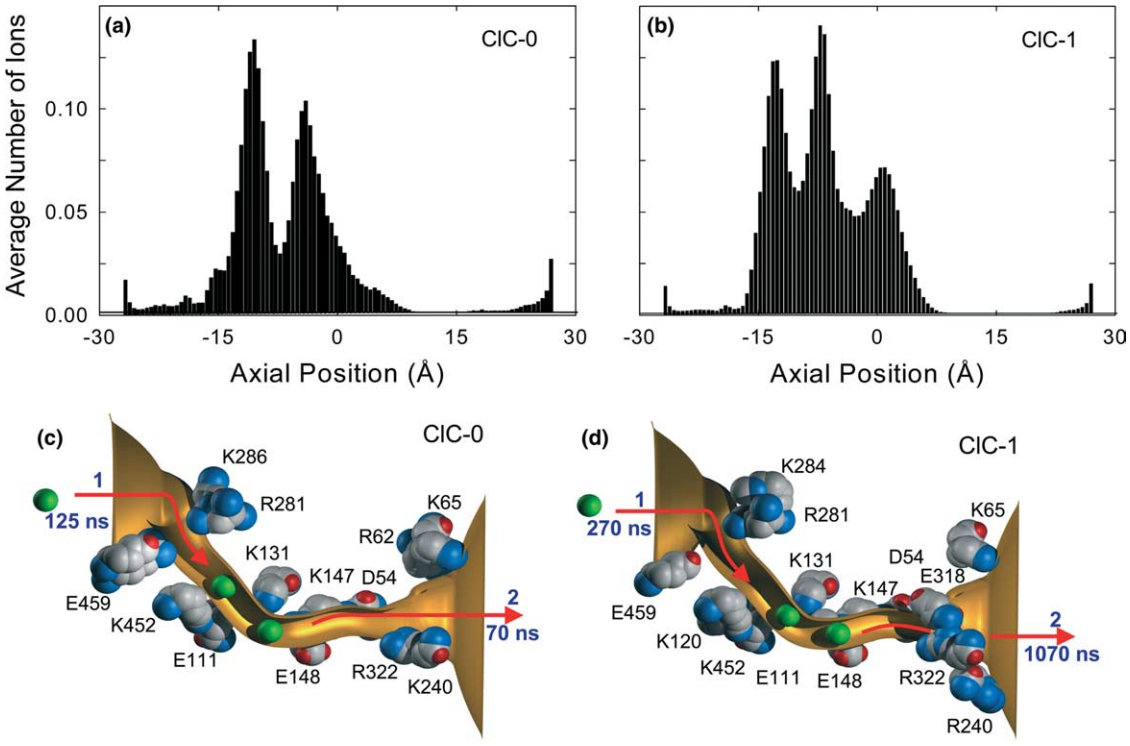

Fig. 4. Dwell histograms and analysis of permeation processes. The distribution of ions in layers of ClC-0 (a) and ClC-1 (b) are derived from Brownian dynamics simulations in the presence of the applied potential of −80 mV. The steps involved and the average time taken in the permeation of Cl^- ions from inside the cell to out (under −80 mV applied potential), and the location of the charged pore lining residues are schematically illustrated for ClC-0 (c) and ClC-1 (d). For ClC-0 the majority of the conduction time is spent waiting for the outermost ion to pass Glu ~ 148 and Asp ~ 54. For ClC-1 this takes longer as the ion also has to pass Glu 318.

additional glutamate residue, Glu 318, lining the pore in ClC-1 as shown in Fig. 4d, whose negative charge slows the transport of cations. This glutamate residue may also make it difficult for a Cl^- to enter from the extracellular reservoir, accounting for the pronounced rectification of ClC-1.

In building our models, we assume that the open-state shape of the prokaryotic ClC channel is the same as that for ClC-0 and ClC-1, and that the structural features that confer specific characteristics of each ClC isoform are the polar and charged amino acid residues near the pore. The three-dimensional atomic models of ClC-0 and ClC-1 we constructed successfully reproduce the experimentally observed conductances and the shape of the current–voltage relationships as well as highlighting the differences in the detailed mechanism of ion permeation in these channels. These differences can be largely attributed to several key amino acid residues. The models we create should be viewed as approximate representations of the open states of the ClC channel isoforms. Although we cannot claim to have replicated the exact atomic positions of the open channels, the success of our models in replicating the available experimental data suggest that we are capturing some of the salient properties of these channels. The success of our technique has prompted us to carry out a series of theoretical site-directed mutagenesis in our model and ascertain which residues need to be mutated to convert ClC-1 to ClC-0 or to enormously enhance the magnitude of currents flowing across the pores. Thus, in studying the family of ClC channels, there can now be a fruitful interaction between theory and experiment, the former making testable predictions and the latter providing clues for further refinements of the model.

Acknowledgements

We thank Dr. David K. Bisset for creating an open-state structure of the EcClC channel. This work was supported by grants from the Australian Research Council and the National Health and Medical Research Council of Australia. The calculations upon which this work is based were carried out using the Compaq AlphaServer SC of the ANU Supercomputer Facility.

References

[1] T.J. Jentsch, T. Friedrich, A. Schriever, H. Yamada, Pflügers Arch. 437 (1999) 783.
[2] M. Maduke, C. Miller, J.A. Mindell, Ann. Rev. Biophys. Biomol. Struct. 29 (2000) 411.
[3] C. Fahlke, Am. J. Physiol. Renal Physiol. 280 (2001) F748.
[4] C. Miller, Philos. Trans. Roy. Soc. Lond. B 299 (1982) 401.
[5] K. Steinmeyer, R. Klocke, C. Ortland, M. Gronemeier, H. Jockusch, S. GrÃ¦nder, T.J. Jentsch, Nature 354 (1991) 304.
[6] M.C. Koch, K. Steinmeyer, C. Lorenz, K. Ricker, F. Wolf, M. Otto, B. Zoll, F. Lehmann-Horn, K.H. Grzeschik, T.J. Jentsch, Science 257 (1992) 797.
[7] Y.T. Chen, C. Miller, J. Gen. Physiol. 108 (1996) 237.
[8] M. Pusch, U. Ludewig, A. Rehfeldt, T.J. Jentsch, Nature 373 (1995) 527.
[9] G.Y. Rychkov, M. Pusch, M.L. Roberts, A.H. Bretag, J. Physiol. 530 (3) (2001) 379.
[10] R. Dutzler, E.B. Campbell, M. Cadene, B.T. Chait, R. MacKinnon, Nature 415 (2002) 287.
[11] R. Dutzler, E.B. Campbell, R. MacKinnon, Science 300 (2003) 108.
[12] B. Bennetts, M.L. Roberts, A.H. Bretag, G.Y. Rychkov, J. Physiol. 535 (1) (2001) 93.
[13] R. Estévez, B.C. Schroeder, A. Accardi, T.J. Jentsch, M. Pusch, Neuron. 38 (2003) 47.
[14] J.D. Thompson, D.G. Higgins, T.J. Gibson, Nucleic Acids Res. 22 (1994) 4673.
[15] G. Moy, B. Corry, S. Kuyucak, S.H. Chung, Biophys. J. 78 (2000) 2349.
[16] T. Allen, S.H. Chung, Biochim. Biophys. Acta - Biomembranes. 1515 (2001) 3.
[17] B. Corry, T.W. Allen, S. Kuyucak, S.H. Chung, Biophys. J. 80 (2001) 195.
[18] S.H. Chung, M. Hoyles, T.W. Allen, S. Kuyucak, Biophys. J. 75 (1998) 793.
[19] T.W. Allen, S.H. Chung, Biochim. Biophys. Acta. 1515 (2001) 83.
[20] C. Fahlke, R. Rüdel, N. Mitrovic, M. Zhou, A.L. George, Neuron 15 (1995) 463.
[21] C. Fahlke, C.L. Beck, A.L. George, Proc. Natl. Acad. Sci. USA 94 (1997) 2729.
[22] C. Saviane, F. Conti, M. Pusch, J. Gen. Physiol. 113 (1999) 457.
[23] F. Weinreich, T.J. Jentsch, J. Biol. Chem. 276 (2001) 2347.